Electronic Supplementary Material (ESI) for Dalton Transactions.

Synthesis of Carbon-wrapped Microsphere MoO_2/Mo_2C Heterojunction as Efficient Electrocatalysts for Oxygen Reduction Reaction and Hydrogen Evolution Reaction

Jiannan Cai[a], Xiaofeng Zhang[bc], Ting Wang[bc], Yuande Shi[a*], Shen Lin[bc*]

a Fujian Polytechnic Normal University, Fuzhou, China, 350300

b College of Chemistry & Materials Science, Fujian Normal University, Fuzhou 350007, China

c Fujian Provincial Key Laboratory of Advanced Materials Oriented Chemical Engineering, Fuzhou 350007, China

*Corresponding author

E-mail address: asw19931126@163.com (Jiannan Cai), shenlin@fjnu.edu.cn (Shen Lin)

1 Experimental

1.1 Chemicals

Ammonium molybdate tetrahydrate ($(NH_4)_6Mo_7O_{24}\cdot 4H_2O$), β-cyclodextrin, Vulcan XC-72R(VC), ethanol absolute (C_2H_5OH), potassium hydroxide (KOH) and methanol (CH_3OH) were of analytical grade and from Sinopharm Chemical Reagent Co., Ltd. A commercial 20 wt% Pt/C catalyst was purchased from Alfa Aesar. A Nafion solution (5 wt% in a mixture of lower aliphatic alcohols and water) was purchased from Sigma-Aldrich. High-purity oxygen (O_2, 99.999%) and nitrogen (N_2, 99.999%) were sourced from Huaxinda Industrial Gas Co., Ltd.

1.2 Characterizations

XRD was carried out using an X-ray diffractometer (X'Pert PRO) in the 5°-90° range. XPS was done on an Escalab 250Xi X-ray photoelectron spectrometer with Al Kα as M-SRRPS (Microstrip Slit-Ring Resonator Plasma Source). The method of energy calibration is a charged correction, using 284.6 eV as standard value to calibrate C1s spectra. According to the difference of C1s spectra, then all the XPS spectra of the remaining elements rose or fell to a certain value. Then XPS peak software was implemented to analyze the data. The steps are importing data, establishing baseline, adding peak (according to references), adjusting parameters (FWHM 0.5–3.5eV, the area of peak). The Raman spectrometer (Thermo Fisher DXR) reported a wavelength of 532 nm. The scanning electron microscopy (SEM) images were measured using a scanning electron microscope (JSM-7500F, 5 KV). The transmission electron microscopy (TEM) was operated by Tecnai-G20 TEM at an acceleration voltage of 200 KV. The high-resolution transmission electron microscopy (HRTEM) images were obtained by Tecnai G20 HRTEM. Using Inductively coupled plasma spectromete (ICP) to test the Mo content of powder and electrolyte.

1.3 Synthesis of the $MoO_2/Mo_2C/C$ composite

The microsphere $MoO_2/Mo_2C/C$ heterojunction materials was synthesized by the following steps. Firstly, 1.0 g ammonium molybdate tetrahydrate ($(NH_4)_2MoO_4\cdot 5H_2$), 2.0 g β-cyclodextrin and 50 mg Vulcan XC-72R were added into 25 ml deionized water. Above mixture was stirred for 8 h at room temperature. Then the mixture solutions were transferred into 100 ml Teflon-lined stainless steel autoclaves and heated at 200 °C for 24 h. After the hydrothermal reaction, black material was prepared via centrifugal washing 3 times for ten minutes each time by ethanol and deionized water each and vacuum dried at 65 °C. Finally, black material was calcined in Ar atmosphere at 400 °C for 1 h and following 800 °C for 2 h. When cooled to room temperature, they were taken out and centrifugally washed 3 times for ten minutes each time by ethanol and deionized water, respectively. The titled product were dried and milled to be used for the next tests. The contrasting MoO_2/Mo_2C samples were synthesized by the same method. The amount of ammonium molybdate has 0.5, 1.0, 1.5 and 2.0g, named as $MoO_2/Mo_2C/C$-0.5, $MoO_2/Mo_2C/C$-1.0,

$MoO_2/Mo_2C/C$-1.5, $MoO_2/Mo_2C/C$-2.0.

1.4 Electrochemical measurements

The electrochemical test was measured using a standard three-electrode system (CHI 760E) with a glassy carbon electrode (diameter 5 mm, surface area 0.196 cm^2) as a working electrode, a graphite rod as a counter electrode and a saturated silver chloride electrode with salt bridge as a reference electrode. All potential values were calibrated to the reversible hydrogen electrode: $E_{(RHE)} = E_{(Ag/AgCl)}+0.0592*pH + 0.197$.

The catalysts were preprocessed by following the procedure whereby the glassy carbon electrodes were embellished by the coating method: 5.5 mg MoO_2/Mo_2C, the $MoO_2/Mo_2C/C$ composite and VulcanXC-72R were added into a 3 ml centrifugal tube. Moreover, 450 μL isopropyl alcohol and 50 mL 5% Nafion 117 solution were added. Then the solution was treated by ultrasonication for 1 h to form a homogeneous sample ink. Consequently, 3.6μL ink was dropped on the surface of the GC electrode with a diameter of 4 mm and 10.0 μL ink was dropped on the surface of this electrode having a diameter of 5 mm. The prepared GC electrodes were obtained after cooling to room temperature. The commercial Pt/C was preprocessed utilizing the same method.

ORR test: Linear sweep voltammetry (LSV) was tested on a rotating disk electrode (RDE) at a scanning rate of 10 mv s^{-1} with different rotation rates (400, 625, 900, 1225, 1600, 2025 rpm), and the electrolyte was a 0.1 M KOH solution saturated with O_2 or N_2 (just 225 rpm) that must be purged over 40 min.

The rotating ring-disk electrode technique (RRDE, 1600 rpm) was measured to verify the electrons transfer number n, and to obtain the yield of H_2O_2 for ORR. The value of n and the yield of H_2O_2 were obtained by the following formulas:

$$n = 4I_D/(I_D + I_R/N) \quad (1)$$

$$H_2O_2\% = 200I_R/(NI_D + I_R) \quad (2)$$

Where: I_D is the test current of disk; I_R denotes the test current of the ring; and N stands for the collection efficiency (0.37) . The accelerated durability test was carried out using CV between 0.6 and 1.2 V (RHE) with 50 mV s^{-1} for 1000 cycles. When testing for changes in the structural composition after catalysis, it was used Indium Tin Oxides electrically conductive glass (ITO) as working electrode (10ml 0.1 M KOH as electrolyte and using 100 μL ink dropped on the surface of ITO). Furthermore, the chronoamperometry was tested at the CV peak potential of ORR with 20000 s and 12 h.

HER test: The electrochemical measurements of HER were conducted in 1 M KOH aqueous solutions for electrolyte at room temperature. ① The cyclic voltammetry (CV) curves test method: 1 M KOH aqueous solutions were saturated by bubbling N_2 for 45 minutes. Then a three-electrode configuration, glassy carbon electrode with green electrode wire as work electrode, saturated Hg/HgO electrode with white electrode wire as reference electrode and graphite with red electrode wire as the counter electrode were put into the electrolyte together. The voltage ranged from - 0.8 to - 0.5 V with scan rates from 10 to 100 V mV s^{-1} in CV measurements to obtain electrochemical surface area (ECSA). The ECSA of electrocatalysts were

obtained by double-layer capacitance using the following formula:

$$ECSA=C_{DL}/C_s \quad (3)$$

$$i_c=vC_D \quad (4)$$

C_s was 0.040 mF/cm^2 with the 1 M KOH aqueous solutions, i_c was double-layer charge current of non-apparent Faraday potential and v scan rates in the formula. The saturated Hg/HgO reference electrodes were calibrated with respect to the reversible hydrogen electrode using at room temperature: $E_{(RHE)} = E_{(Hg/HgO)} +0.098 +0.0592*$ pH.

② The Linear sweep voltammetry (LSV) curves of the HER test method: 1 M KOH aqueous solutions and three-electrode configuration were processed by the same method as done in ①. The scanning rate was identical in the LSV and CV test, respectively. The voltage range was from -1.6 to -0.8V and rotating speed was 1600 rpm versus RHE in LSV measurements to obtain LSV curves in a nitrogen-saturated electrolyte. Tafel slope was obtained by the Tafel formula written as follows:

$$\eta=a+b\cdot\log J \quad (5)$$

η was overpotential, J was current density after normalizing the geometric surface area of glassy carbon electrodes and b was Tafel slope in the formula.

③ Continuous Cyclic voltammograms test method: the continuous Cyclic voltammograms were produced in a nitrogen-saturated 1M KOH solution with scan range from -1.2 to - 0.8V, scan rate for 10 mV s^{-1}, scanning 1000 times and 2000 times, respectively. ④ Chronopotential (E-T）curves test method: the chronopotential curves were produced in a nitrogen-saturated 1M KOH solution with measuring parameter for 10 mA/cm^2, scanning time for 10 h. ⑤Chronoamperometry (I-T) curves test method: the chronoamperometry curves were produced in a nitrogen-saturated 1M KOH solution with scanning time for 10 h, beginning at the current density for mA cm^{-2}.

Turn over frequency (TOF) was measure Mo as the main active centers. The formula is as follows：

$$TOF_{Mo}(s^{-1}) = [J \times Mw/ (4F \times m \times x)]$$

where J is current density , Mw is the molar mass of Mo, m is the actual mass of the catalyst, F is Faraday constant, and x is the mass percentage of Mo (ICP).

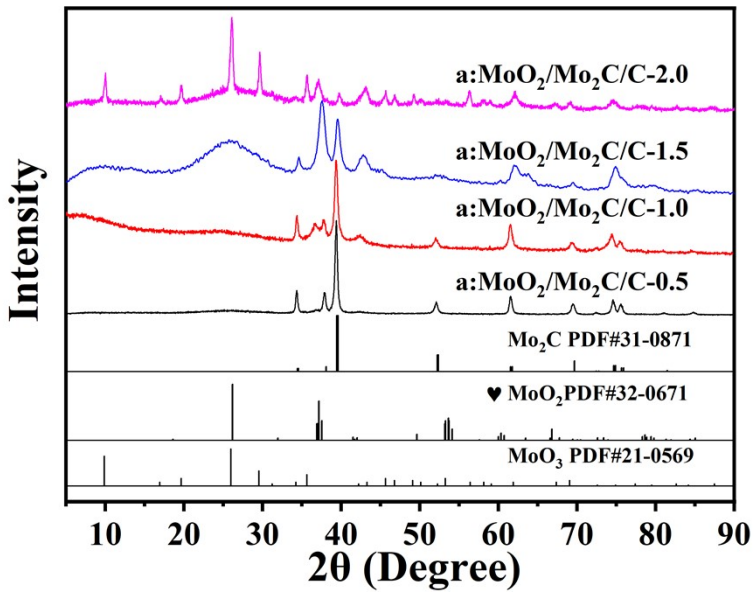

Fig. S1 XRD of catalysts using the different amount of ammonium molybdate

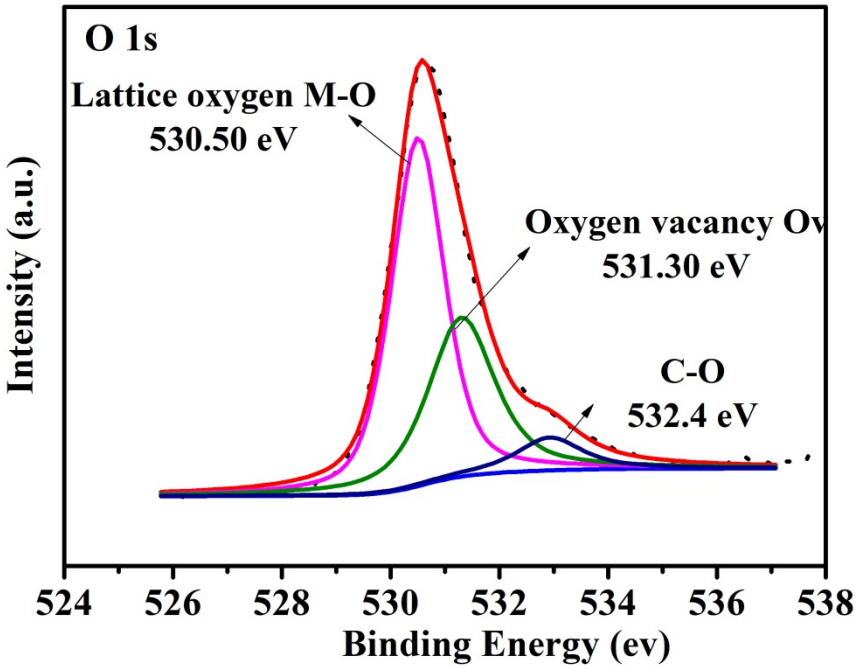

Fig. S2 XPS spectra of $MoO_2/Mo_2C/C$: O 1s spectrum

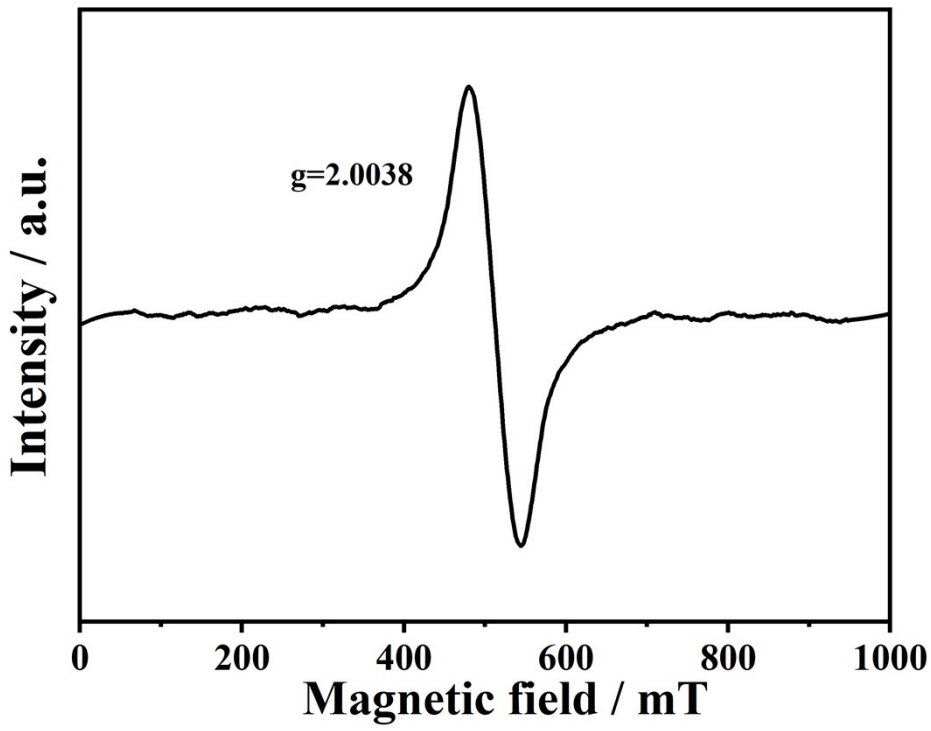

Fig. S3 The EPR of $MoO_2/Mo_2C/C$

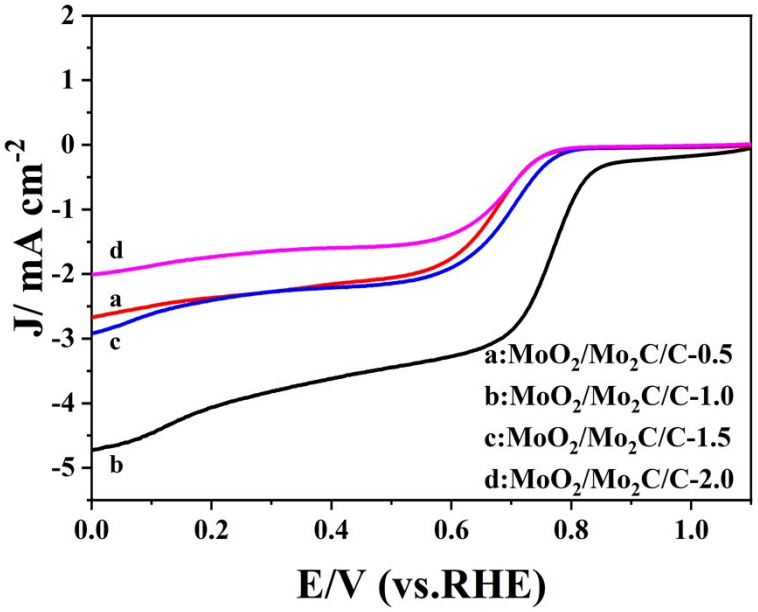

Fig.S4 The LSV curves of catalysts using the different amount of ammonium molybdate toward ORR

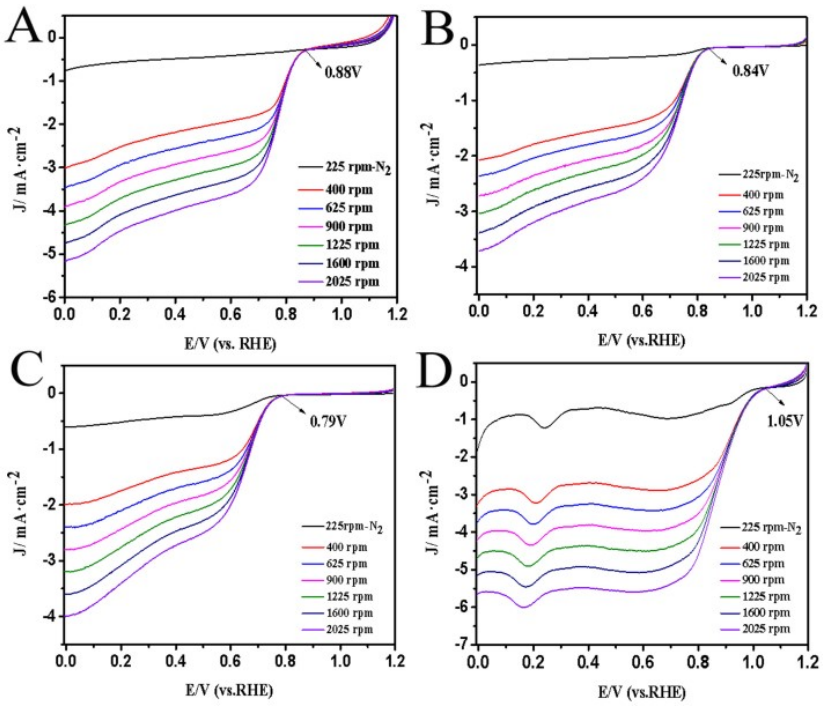

Fig. S5 LSV curves of $MoO_2/Mo_2C/C$ (A), MoO_2/Mo_2C (B), Vulcan XC-72R (C) and Pt/C (D) at different rotation rates in ORR.

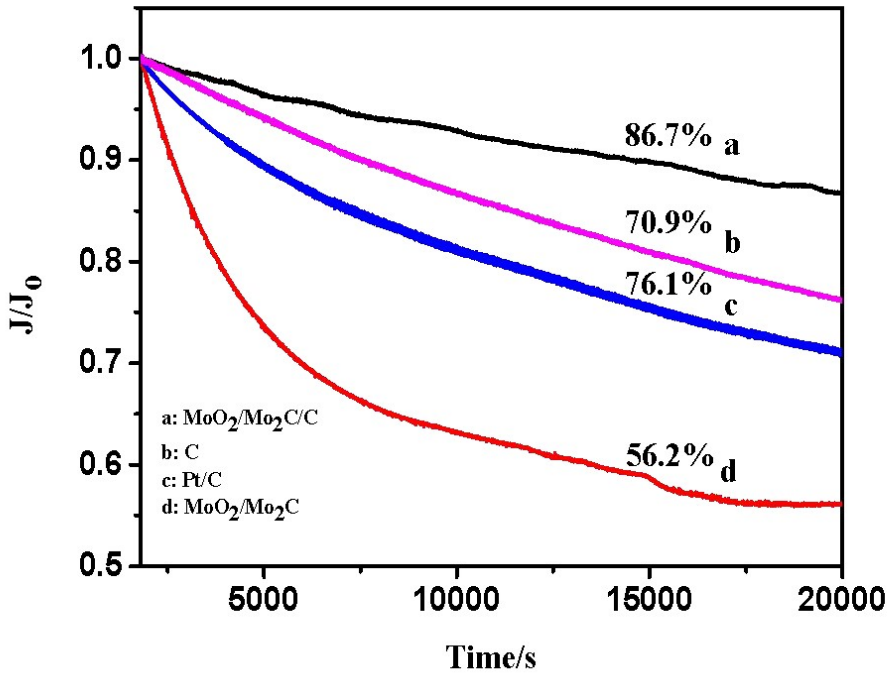

Fig. S6 Chronoamperometric curves for the $MoO_2/Mo_2C/C$ (a), Vulcan XC-72R (b), Pt/C (c), MoO_2/Mo_2C (d) for 20000 s at 0.77V vs. RHE.

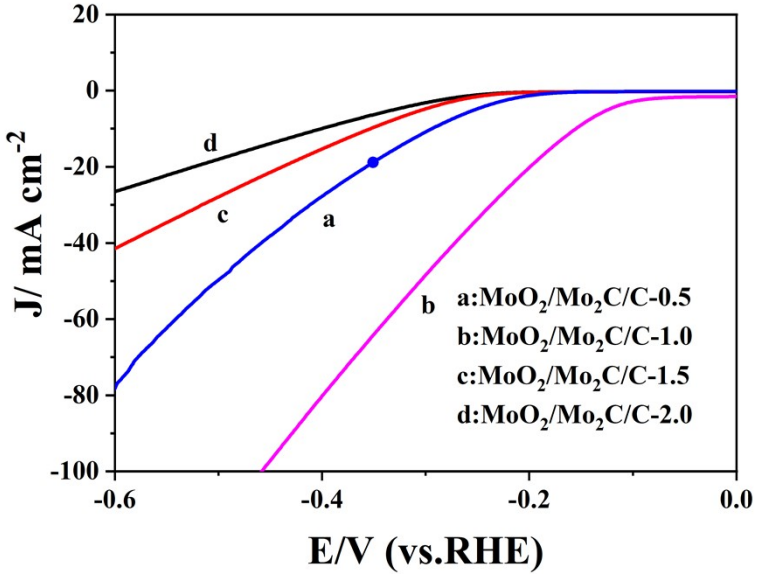

Fig.S7 The LSV curves of catalysts using the different amount of ammonium molybdate toward HER

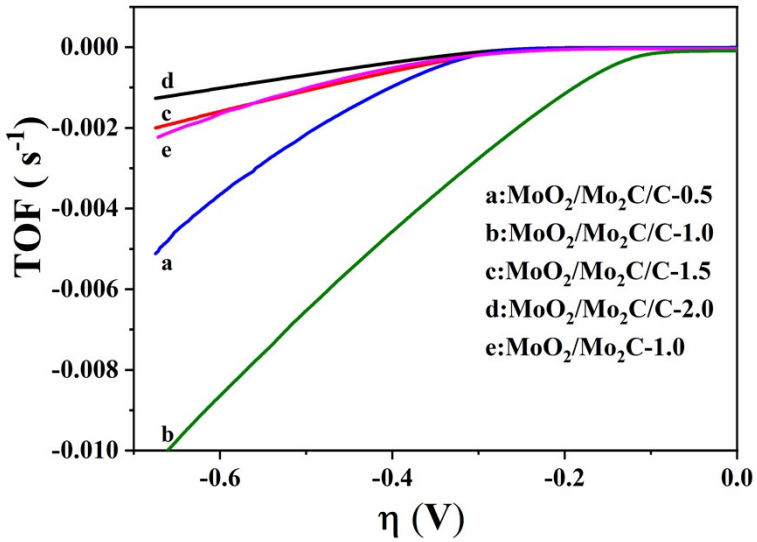

Fig. S8 TOFs of catalysts toward HER

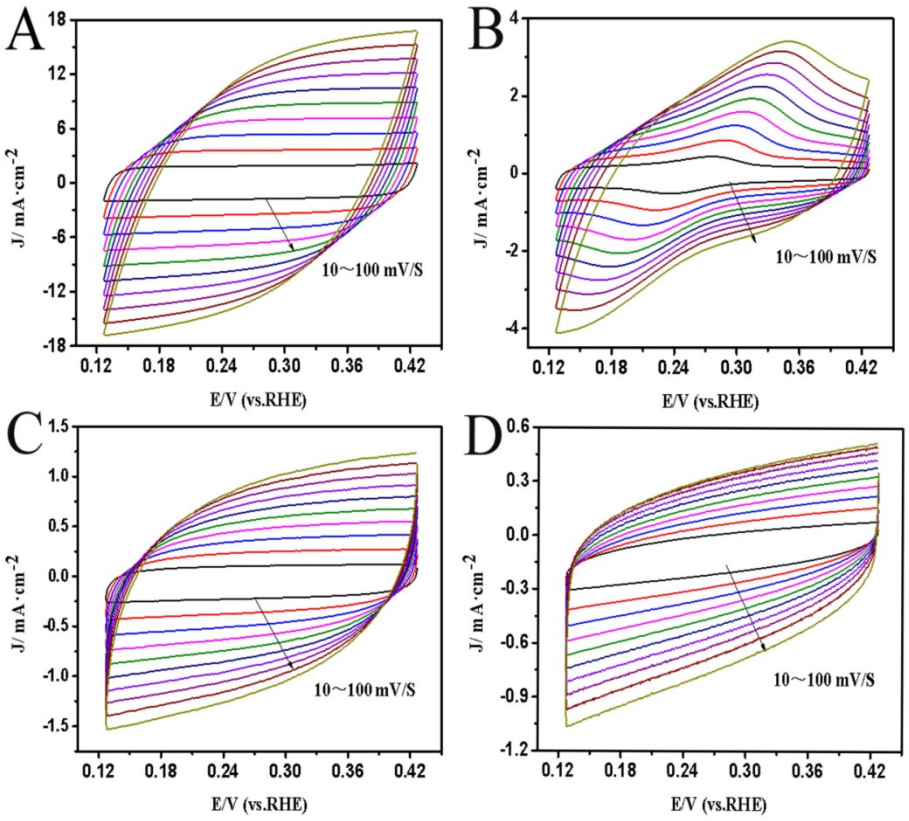

Fig. S9 CV curves of $MoO_2/Mo_2C/C$ (A), Pt/C (B), MoO_2/Mo_2C (C) and Vulcan XC-72R (D).

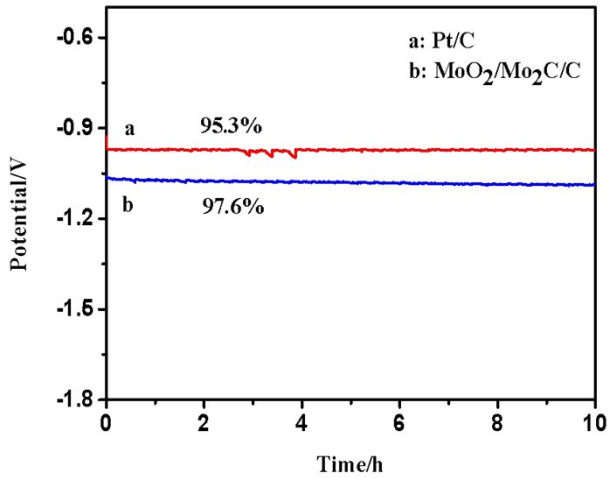

Fig. S10 Chronopotentiometric curves of Pt/C (a) and $MoO_2/Mo_2C/C$ (b) after scanning 10 h

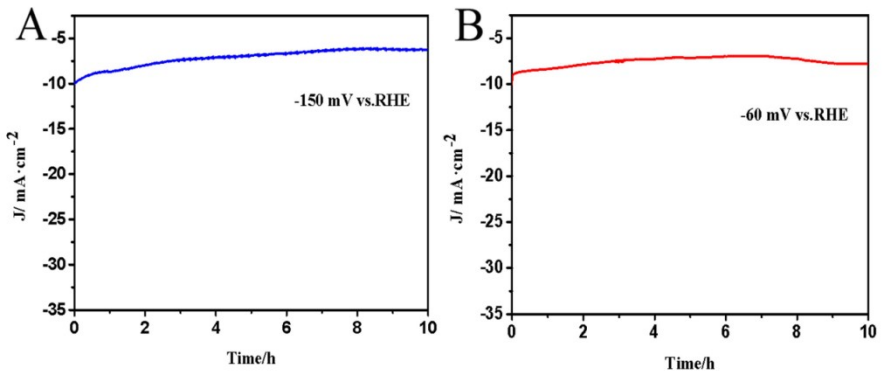

Fig. S11 Chronoamperometric curves of $MoO_2/Mo_2C/C$ (A) and Pt/C (B) in N_2-saturated 1 M KOH solution for 10 h at a current density of 10 mA cm^{-2} with -150 mV (vs.RHE) and -60 mV (vs.RHE), respectively.

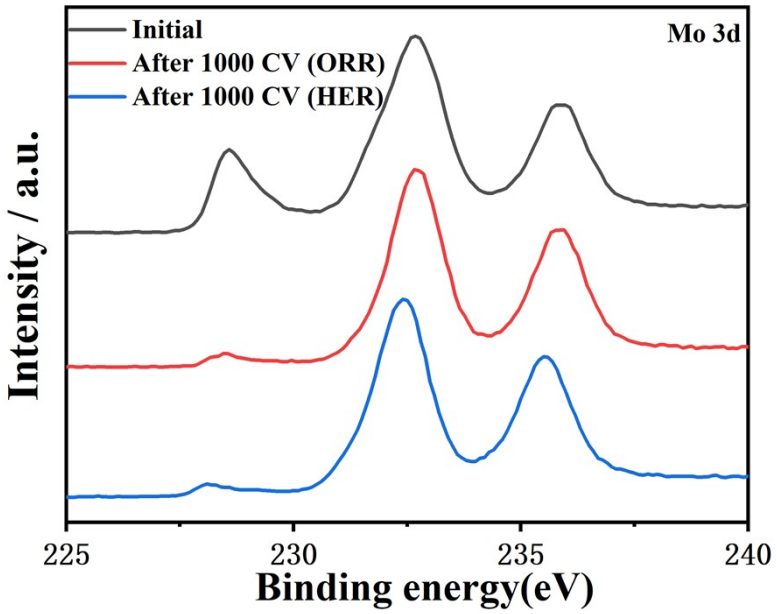

Fig. S12 The Mo3d spectrogram of $MoO_2/Mo_2C/C$ before and after 1000 CV cycles toward ORR and HER

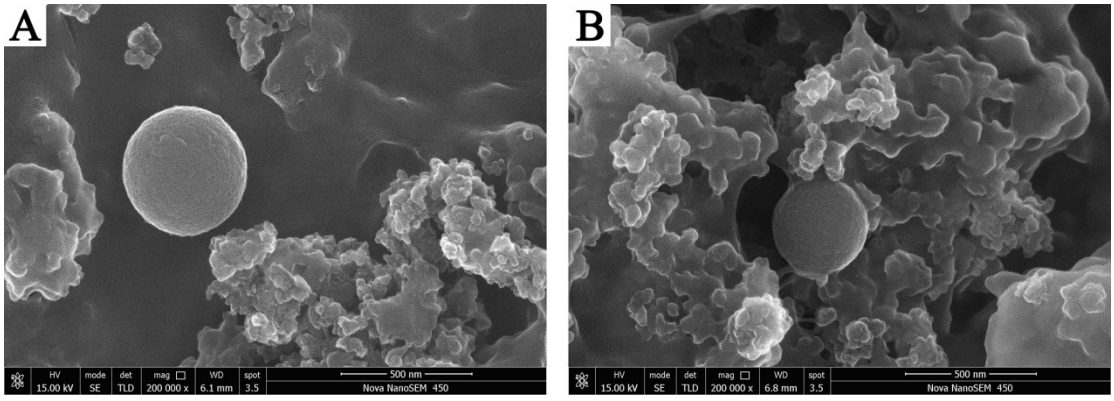

Fig. S13 The SEM images of $MoO_2/Mo_2C/C$ after 1000 CV cycles toward ORR(A) and HER(B)

Table S1. Comparison of ORR activity of $MoO_2/Mo_2C/C$ with other ORR catalysts reported before.

Number	Catalyst	$E_{1/2}$/V	Electrolyte	Ref
1	$MoO_2/Mo_2C/C$	**0.74**	**0.1M KOH**	**This work**
2	P-MoO_2	0.72	**0.1M KOH**	[1]
3	Hierarchical Mo-based nanospheres(HNs)	0.751	**0.1M KOH**	[2]
4	N-MoO_2-Mo_2C	0.70	0.1M KOH	[3]
5	Mo_2C/NCNT-30	0.62	0.1 M KOH	[4]
6	MoC/MoS_2	0.64	0.1 M KOH	[5]
7	CoP-PBSCF	0.75	0.1M KOH	[6]
8	Co@NPC-H	0.77	0.1M KOH	[7]
9	A-PBCCF-H	0.76	0.1M KOH	[8]
10	MoO_3/NG	0.748	0.1M KOH	[9]
11	MoO_2/C-30	0.62	0.1M KOH	[10]

Table S2. Comparison of HER activity of $MoO_2/Mo_2C/C$ with other HER catalysts reported before.

Number	Catalyst	Overpotentail / mV ($J_{=10}$)	Electrolyte	Ref
1	$MoO_2/Mo_2C/C$	**150**	**1M KOH**	**This work**
2	**20% Pt/C**	**60**	**1M KOH**	**This work**
3	MoO_2/MoC_2	161	1M KOH	[11]
4	Co/Mo_2C-NCNTs	170	1 M KOH	[12]
5	$Ni-Mo_2C$@NPC	183	1 M KOH	[13]
6	$Fe_5C_2-Fe_3C$@C	209	1M KOH	[14]
7	$Ni_3Se_2/NiSe$	198	1M KOH	[15]
8	$MoS_2/Co-N-CN_2$	180	1M KOH	[16]
9	CoP@SNC	174	1M KOH	[17]
10	Co_3O_4/MoS_2	205	1M KOH	[18]
11	$NiSe_2$@NG	248	1M KOH	[19]
12	annealed-MoS_2/rGO	154.77	1M KOH	[20]
12	Co_3O_4@MoO_3	158	1M KOH	[21]

Tables S3. The ratio of Mo in catalysts

	The ratio of Mo (%)
$MoO_2/Mo_2C/C$-2.0	51.7
$MoO_2/Mo_2C/C$-1.5	52.2
$MoO_2/Mo_2C/C$-1.0	34.7
$MoO_2/Mo_2C/C$-0.5	30.5
MoO_2/Mo_2C-1.0	43.4

Tables S4. The amounts of dissolved Mo elements in 10 mL electrolyte

	Concentration of Mo(mg L^{-1})	The amounts of dissolved Mo (mg)
ORR	1.0812	0.010812
HER	1.2262	0.012262

Reference

1. X. Cui, Y. Tao, X. Xu and G. Yang, *J. Power Sources*, 2023, **557**, 232519.
2. Q. Li, D. Kong, G. Yang, Y. Cai, Q. Pan, F. Zheng, Z. Ma and H. Wang, *Catalysis Science & Technology*, 2020, **10**, 6713-6722.
3. L. Karuppasamy, L. Gurusamy, S. Anandan, C.-H. Liu and J. Wu, *Materials Today Chemistry*, 2022, **24**, 100799.
4. Y.-J. Song, J.-T. Ren, G. Yuan, Y. Yao, X. Liu and Z.-Y. Yuan, *Journal of Energy Chemistry*, 2019, **38**, 68-77.
5. Y. Li, S. Zuo, X. Wu, Q. Li, J. Zhang, H. Zhang and J. Zhang, *Small*, 2021, **17**, 2003256.
6. Y.-Q. Zhang, H.-B. Tao, Z. Chen, M. Li, Y.-F. Sun, B. Hua and J.-L. Luo, *Journal of Materials Chemistry A*, 2019, **7**, 26607-26617.
7. Y.-N. Hou, Z. Zhao, H. Zhang, C. Zhao, X. Liu, Y. Tang, Z. Gao, X. Wang and J. Qiu, *Carbon*, 2019, **144**, 492-499.
8. B. Hua, M. Li, Y.-F. Sun, Y.-Q. Zhang, N. Yan, J. Chen, T. Thundat, J. Li and J.-L. Luo, *Nano Energy*, 2017, **32**, 247-254.
9. K. Maiti, N. Kim and J. Lee, *Chemical Engineering Journal*, 2021, **410**, 128358.
10. W. Liu, J. Cai, B. Huang, X.-f. Zhang and S. Lin, *New J. Chem.,*, 2021, **45**, 7417.
11. R. Zhang, X. Xiao, Z. Wang, J. Huang, Z. Wang, Y. Dong and J. Liu, *Mater. Lett.*, 2021, **297**, 129973.
12. J. Zhang, X. P. Sun, P. Wei, G. Lu, S. X. Sun, Y. Xu, C. Fang, Q. Li and J. T. Han, *ChemCatChem*, 2020, **12**, 3737-3745.
13. Y. Lu, C. Yue, Y. Li, W. Bao, X. Guo, W. Yang, Z. Liu, P. Jiang, W. Yan and S. Liu, *Applied Catalysis B: Environmental*, 2021, **296**, 120336.
14. Z. Ye, Y. Qie, Z. Fan, Y. Liu, Z. Shi and H. Yang, *Dalton Trans.*, 2019, **48**, 4636-4642.
15. H.-B. Wang, Y.-S. Sun, F. Ma, L. Zhou, H.-F. Li, L. Zhang, G.-J. Chen, Y.-K. Xu, Y.-N. Chen and K.-W. Xu, *J. Alloys Compd.*, 2020, **819**, 153056.
16. X. Hou, H. Zhou, M. Zhao, Y. Cai and Q. Wei, *ACS Sustainable Chemistry & Engineering*, 2020, **8**, 5724-5733.
17. T. Meng, Y.-N. Hao, L. Zheng and M. Cao, *Nanoscale*, 2018, **10**, 14613-14626.
18. A. Muthurasu, V. Maruthapandian and H. Y. Kim, *Applied Catalysis B: Environmental*, 2019, **248**, 202-210.
19. W. Li, B. Yu, Y. Hu, X. Wang, D. Yang and Y. Chen, *ACS Sustainable Chemistry & Engineering*, 2019, **7**, 4351-4359.
20. W. Dong, H. Liu, X. Liu, H. Wang, X. Li and L. Tian, *Int. J. Hydrogen Energy*, 2021, **46**, 9360-9370.
21. C. Zhang, Y. Liu, J. Wang, W. Li, Y. Wang, G. Qin and Z. Lv, *Applications of Surface Science*, 2022, **595**, 153532.